Investigation on effect of welding parameters on solidification cracking of austenitic stainless steel 314

Citation for the original published paper (version of record):
Singh, S., Hurtig, K., Andersson, J. (2018). Investigation on effect of welding parameters on
solidification cracking of austenitic
stainless steel 314. Procedia Manufacturing, 25: 351-357.
http://dx.doi.org/10.1016/j.promfg.2018.06.103

Available online at www.sciencedirect.com

ScienceDirect

Procedia Manufacturing 25 (2018) 351–357

Procedia MANUFACTURING

www.elsevier.com/locate/procedia

8th Swedish Production Symposium, SPS 2018, 16-18 May 2018, Stockholm, Sweden

Investigation on effect of welding parameters on solidification cracking of austenitic stainless steel 314

Sukhdeep Singh[a] *, Kjell Hurtig[b], Joel Andersson[b]

[a]*Department of Industrial and Materials Science, Chalmers University of Technology, Gothenburg SE-412 96, Sweden*
[b]*Department of Engineering Science, University West,Gustava Melins gata 2*
S-461 32 Trollhättan, Sweden

Abstract

This study investigates the solidification cracking susceptibility of the austenitic stainless steel 314. Longitudinal Varestraint testing was used with three different set of welding test parameters. Weld speed, current and voltage values were selected so that the same heat input resulted in all the test conditions. From the crack measurements it was seen that the test condition with the lowest current and welding speed value also produced the least amount of cracking with very good repeatability.

Peer-review under responsibility of the scientific committee of the 8th Swedish Production Symposium.

Keywords: Solidification cracking; Steel 314; Varestraint testing; Welding parametres.

1. Introduction

Austenitic stainless steels are widely used, especially when it comes to high temperature applications where strength, oxidation and corrosion aspects are of concern. The austenitic stainless steel 314, also designated as EN 1.4841, was specifically developed for increased temperature resistance [1] and its application can be found in e.g. superheater tubes for boiler plants. These superheaters are made out of multiple tubes which are joined together by

* Corresponding author. Tel.: +46520223207
E-mail address: sukhdeep.singh@chalmers.se

2351-9789
Peer-review under responsibility of the scientific committee of the 8th Swedish Production Symposium.
10.1016/j.promfg.2018.06.103

welding. Welding defects categorized as hot cracks can occur under high restraint conditions, where specifically the austenitic stainless steels are prone to solidification cracks, a type of cracking which occurs in the fusion zone. Solidification cracks occur during the final stage of the weld metal solidification due to the reduced ductility at the grain boundaries by the presence of liquid films [2], [3]. The extent of cracking is often related to the welding parametres, therefore, a DOE (Design of Expirements) is usually performed in order to find a good compromise between weldability and productivity [4]. The current study investigates the effect of varying welding parametres in relation to the solidification cracking suceptibility of austenitic stainless steel 314 by Varestratint weldability testing method. The welding parametres were selected among a large DOE window range in discussion with the project partners. The aim is to provide data that will be used as reference in selecting welding parametres by the boiler manufacturers.

2. Experimental

The chemical composition in wt % of the 314 austenitic stainless steel can be seen in Table 1.

Table 1. Chemical composition of the austenitic stainless steel 314 in wt%.

C	Si	Mn	P	S	Cr	Mo	Ni	N	Ti
0.057	1.91	1.42	0.024	0.0008	24.27	0.45	19.04	0.030	0.057

Test plates with dimensions of 150 x 50 mm were cut out from a large sheet with 5 mm in thickness and tested in the solution heat treated condition (1050°C followed by air cooling). Three different sets of welding parameters were used with varying current and welding speed while maintaining constant arc length of 3 mm and the same heat input as per Table 2. Argon shielding gas of 15 l/min was used to protect the welds from oxidation.

Table 2. GTAW (gas tungsten arc welding) test parameters used Varestraint testing.

	Current	Voltage	Speed (mm/min)	Heat Input (KJ/mm)
a	100	10	70	0.8
b	140	10	100	0.8
c	180	10	130	0.8

The three test conditions are hereafter referred to as 100_70, 140_100 and 180_130, respectively. Bead on plate welds were performed by longitudinal Varestraint weldability testing equipment, Figure 1. Figure 2 discloses the details of the test set up. Test plates were positioned on top of the die mandrel. Once the welding reached a steady state condition, bending was performed with the help of two support plates in order to have uniform bending.

Testing was conducted at a fixed augmented strain level of 5% and by using a stroke rate of 1 mm/s. Three test plates were tested for each set of welding parameter. After testing, weld surfaces were cleaned to remove any oxide layers by the use of fine grinding paper. Crack measurements of the top surface of respective specimen were conducted using a stereo microscope. Ferrite measurements in the base metal and weld metal were carried out by using a Feritscope. Sample preparation followed the conventional procedures of manual cutting, mounting, grinding and polishing steps. Samples were etched electrolytically by oxalic acid solution. The samples were over-etched in order to reveal the grain boundaries for grain size measurements. Microstructural investigation was conducted by optical light microscopy. Hardness measurements were conducted by Vickers microhardness test using HV0.5 load.

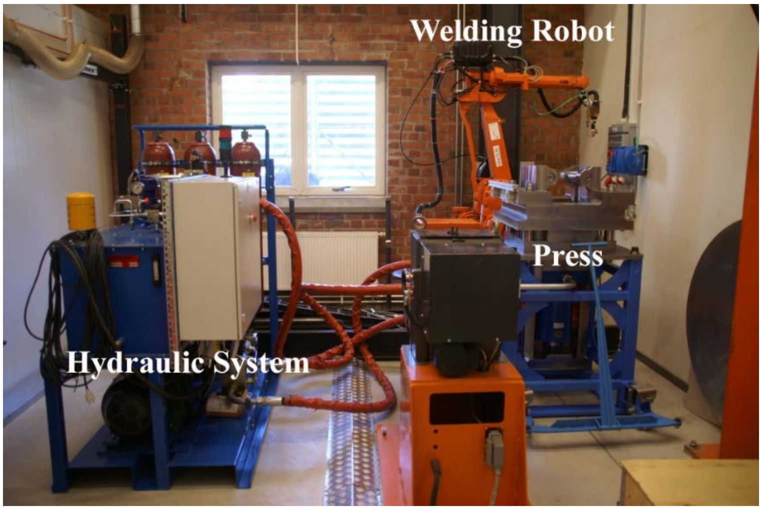

Figure 1. Varestraint weldability testing equipment at University West.

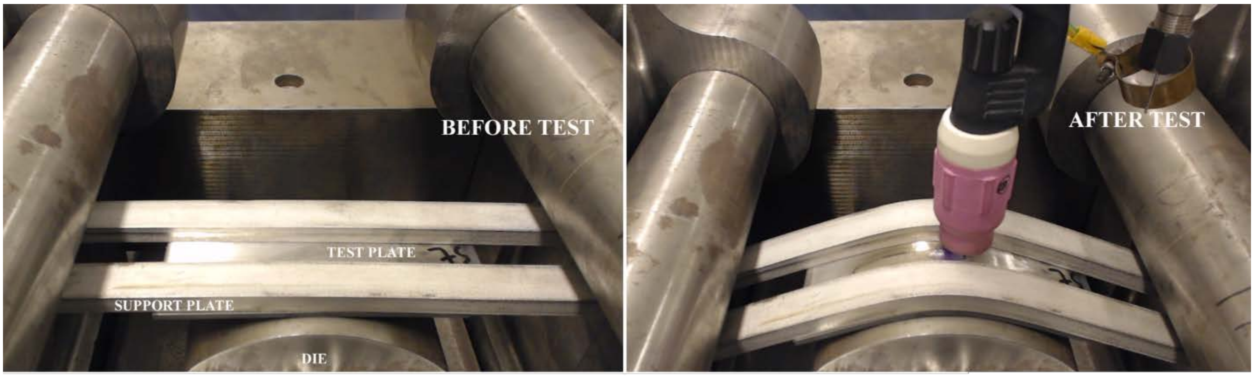

Figure 2. Test set up for the Varestraint test.

3. Results and Discussion

Crack measurements from each test plate are represented in terms of TCL (Total crack length) in Figure 3. It can be seen that the welding condition described as 100_70, where 100 is the welding current and 70 is the welding speed, overall disclosed the lowest amount of cracking of about 2.5 mm with similar values between the three plates. Increasing weld current and welding speed (180_130) resulted in increased amount of cracking with values between 3 and 4 mm. The test condition with intermediate welding current and speed, 140_100, exhibited a relatively high scatter with minimum value of 2.3 mm and maximum 4.1 mm in TCL.

Figure 4 represents the weld profiles with top and transversal views. It can be seen that while the weld penetration was similar for the three test parameters of about 2 mm in depth, the width increased significantly from 6.6 mm for the 100_70 to 10.2 mm for the 180_130 and intermediate value of 8.7 mm for the 180_130. It is also interesting to see the morphology of the cracking, with centerline cracks for the 100_70 and 140_100, whilst the solidification cracks appeared to be transversal to the welding direction in 180_130. Another interesting fact is that cracking started in an earlier stage for the 180_130 as indicated by the dashed line.

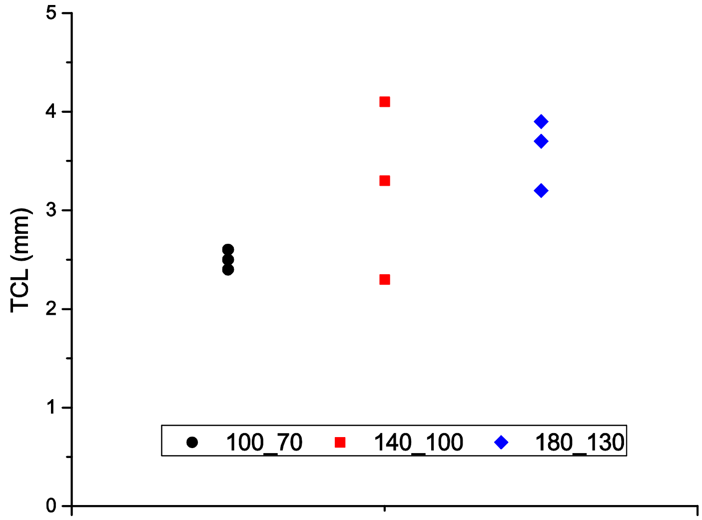

Figure 3. Total crack length values for the solidification cracks at 5% augmented strain.

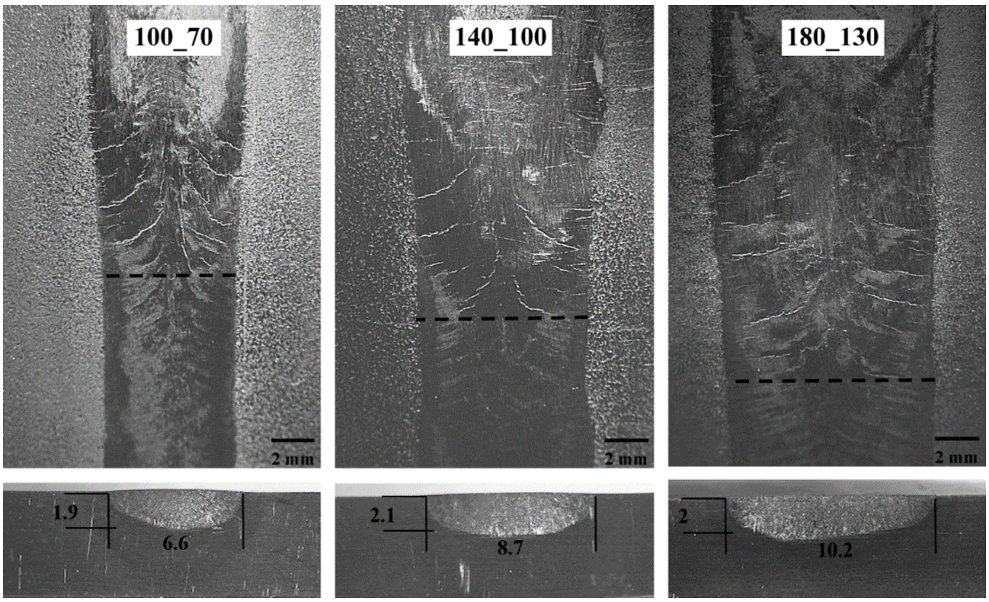

Figure 4. Top and transversal views of the welds including weld bead width and penetration values.

Hardness measurements are presented in Table 3. Similar values of about 190 HV were found for both base metal and fusion zone, while the heat affected zone (HAZ) exhibited a slightly lower value of 170 HV.

Table 3. Average hardness values.

Base Metal	Heat Affected Zone	Fusion Zone
194±3	174±4	189±8

Table 4 represents the ferrite measurements in the base metal and weld metal. The weld length was divided into ten equidistant sections as showed in Figure 5 and ferrite measurements were done in each section from the start to the end of the weld. For each section it was also noted when cracking in the weld metal occurred. Average values in the base metal were 0.2 FN whereas the values in the weld metal varied between 0.2 to 1 FN.

Figure 5. Ferrite measurement locations in the test plate.

Table 4. Ferrite number measurements in the weld metal and base metal.

100_70	WM	BM
Start	0.6	0.2
	0.5	0.2
	0.2	0.2
	0.3	0.2
	0.2	0.2
	0.2	0.2
	0.2	0.1
Crack	0.3	0.2
Crack	0.5	0.2
Stop	0.6	0.1

140_100	WM	BM
Start	0.4	0.2
	0.2	0.2
	0.2	0.2
	0.2	0.2
	0.2	0.2
	0.2	0.2
Crack	0.2	0.2
Crack	0.4	0.2
Crack	0.4	0.2
Stop	2.6	0.2

180_130	WM	BM
Start	0.3	0.2
	0.2	0.2
	0.2	0.2
	0.2	0.2
	0.3	0.2
Crack	0.9	0.2
Crack	1	0.2
Crack	0.9	0.2
Puddle	3.4	0.2
Stop	3.7	0.2

The base metal exhibited a relatively small grain size of 20 µm (ASTM 8), as visible in Figure 6 a). In the HAZ, grain growth occurred, reaching an average value of 90 µm (ASTM 3.5), Figure 6 b).

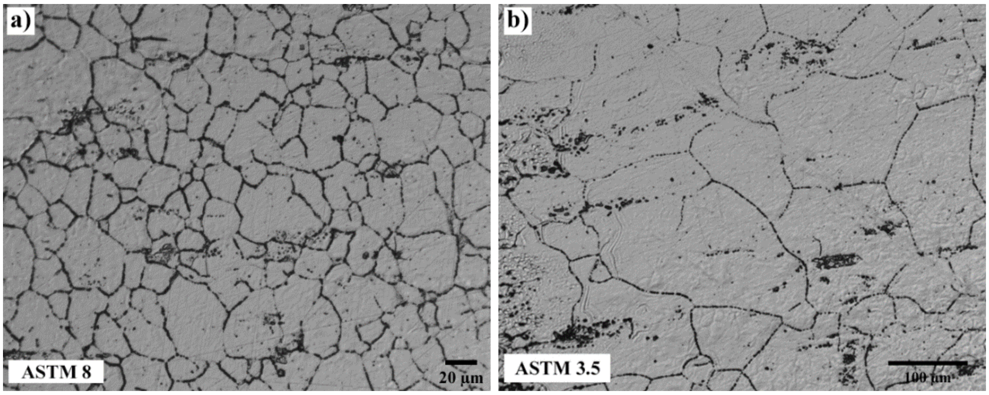

Figure 6. a) Base metal grain size, b) HAZ grain size.

Weld cracking as revealed by light optical microscopy from the 100_70 condition is presented in Figure 7 a). A magnified image of the solidification crack is shown in Figure 7 b).

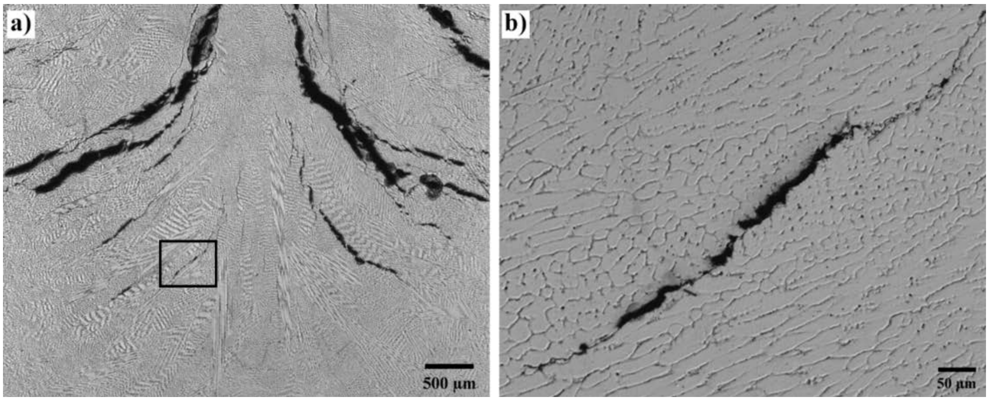

Figure 7. a) Light optical microscope image of solidification cracking, b) cracking occurring along solidification boundary.

4. Discussion

The welds of austenitic stainless steel 314 fall in the fully austenitic mode according to the WRC-1992 diagram [5]. The very low Cr_{eq}/Ni_{eq} of 1.14, where Cr_{eq}=Cr+Mo+0.7Nb=24.72 and Ni_{eq}=Ni+35C+20N+0.25Cu=21.64, makes it highly susceptible to solidification cracking according to Lippold et al. [6]. Ferrite measurements in the weld metal confirm the fully austenitic mode in the welds, the variations in Table 4 are believed to be within the general error range of the measurement technique. It should also be noted that the ferrite measurements in the weld metal may have an influence from the base metal due to the relatively low penetration.

From the results it can be seen that by varying weld current and welding speed while maintaining the same heat input, the amount of cracking is changed. The cracking seems to be related to the depth to width ratio of the weldments: from Figure 4 where it can be seen that the depth remained the same but the width increased with increasing weld current and welding speed, which led to difference in depth to width ratios (D/W). Moreover, as the D/W decreased, the cracking started in earlier stage of bending in relation to higher D/W, as it can be seen from the dashed lines in the same figure and the crack locations in the first columns of Table 4. The D/W for 100_70, 140_100 and 180_130 are, respectively, 0.29, 0.24 and 0.20. It should be noted that there is not a large variation in D/W. Generally, it is preferred to have depth to width ratio of 1:1. Moreover, it was interesting to see the larger scatter in cracking for the 140_100 test condition. Figure 8 shows the different cracking locations in the two test plates, with least cracking (2.3 mm) and the maximum cracking (4.1 mm). These two test plates in Figure 8 a) and b) resemble those of 100_70 and 180_30 in Figure 4. Also note the similarities in the crack locations and morphologies, in Figure 8 a) cracking occurred in the region of maximum bending of the plate, whereas in Figure 8 b) the cracking started at an earlier stage. The large test scatter in the 140_100 condition is therefore believed to be due to the change in the cracking location.

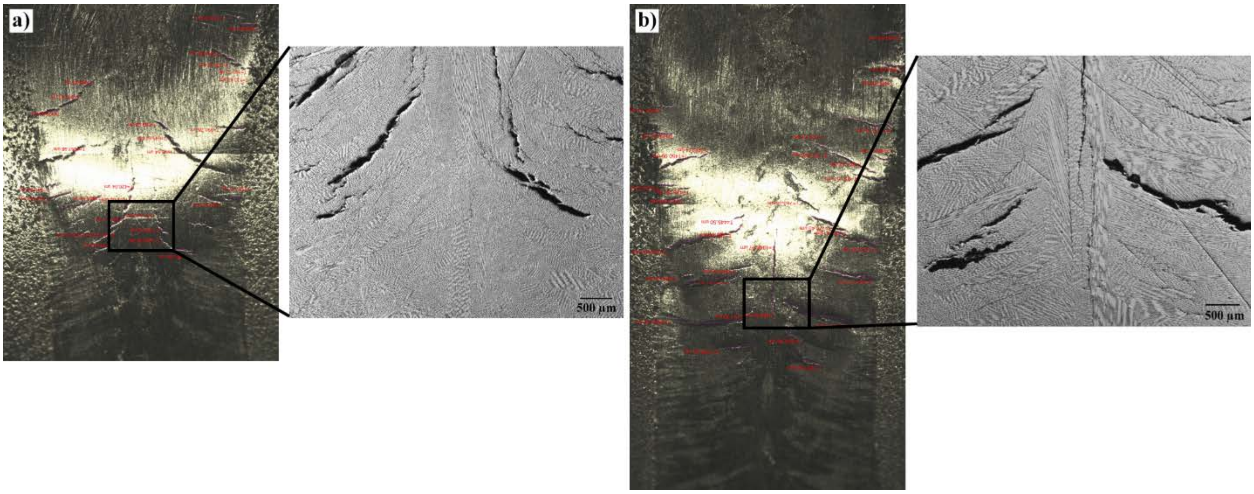

Figure 8. Test plates from the welding parameter of 140_100 a) with the least amount of cracking, b) with the highest amount of cracking.

5. Conclusions

This study shows the influence of the welding parameters on solidification cracking susceptibility. It was seen that the welding parameter set of 100 A in welding current and 70 mm/min in welding speed, disclosed the lowest TCL values as well as smallest variation in TCL among the tested parameters.

Acknowledgements

The authors would like to acknowledge Sumitomo SHI FW for providing the test material. The support from KME through funding from the Swedish Energy Agency and GKN Aerospace Sweden AB is highly appreciated.

References

[1] M. F. McGuire, *Stainless steels for design engineers*. ASM International, 2008.
[2] S. Kou, *Solidification and liquation cracking issues in welding*, JOM, vol. 55, no. 6, pp. 37–42, Jun. 2003.
[3] S. Singh and J. Andersson, *Review of Hot Cracking Phenomena in Austenitic Stainless Steels*, in *7th International Swedish Production Symposium*, 2016, pp. 1–7.
[4] G. M. Goodwin, *The effects of heat input and weld process on hot cracking in stainless steel*, Weld J, vol. 67, p. 88s–94s, 1988.
[5] D. J. Kotecki and T. A. Siewert, *WRC-1992 constitution diagram for stainless steel weld metals: a modification of the WRC-1988 diagram*, Weld. J., vol. 71, no. 5, pp. 171–178, 1992.
[6] J. C. Lippold and D. J. Kotecki, *Welding Metallurgy and Weldability of Stainless Steels*. John Wiley & Sons, 2005.